ELSEVIER

Superlattices and Microstructures 34 (2003) 277–282

Superlattices and Microstructures

www.elsevier.com/locate/superlattices

Discrete dopant effects in ultrasmall fully depleted ballistic SOI MOSFETs

M.J. Gilbert*, D.K. Ferry

Department of Electrical Engineering and Center for Solid State Electronics Research, Arizona State University, Tempe, AZ 85287-5706, USA

Available online 15 June 2004

Abstract

Using a recursive scattering matrix variant, we examine the effects of discrete dopants on the threshold voltage of ultrasmall fully depleted SOI MOSFETs. We find that more highly doped channels produce more interference than do more lightly doped channels. This causes larger fluctuations in threshold voltage. Further, we find that the location of the channel dopants is quite important in the direction of the threshold voltage shift with dopants occurring closer to the source of the device having a larger impact.

For many years the semiconductor industry has been pushing to ever smaller devices. Industry has already demonstrated that it can produce devices that have gate lengths smaller than 15 nm, yet still operate in a normal fashion [1–3]. While the creation of these devices is quite impressive, silicon-on-insulator (SOI) technology has been known to offer better performance over traditional bulk MOSFET devices with better scaling capability. When devices shrink, the method of transport begins to change and quantum phenomena manifest themselves in the active region of these devices. The fact that only a few dopant atoms will exist in the channel of the device creates additional problems. We use a fully quantum mechanical simulation [4] to study the quantum effects of discrete dopants in ballistic, narrow-channel, SOI MOSFETs.

In the channel region of the devices that we consider there are approximately three million silicon atoms. For doping levels of 2×10^{18} and 5×10^{18} cm^{-3}, we expect to see approximately one and two acceptors present in the channel, respectively, for the narrow, thin, and short channels currently under consideration. The dopants themselves are placed

* Corresponding author. Tel.: +1-480-965-3452.
E-mail address: matthew.gilbert@asu.edu (M.J. Gilbert).

0749-6036/$ - see front matter © 2004 Elsevier Ltd. All rights reserved.
doi:10.1016/j.spmi.2004.03.062

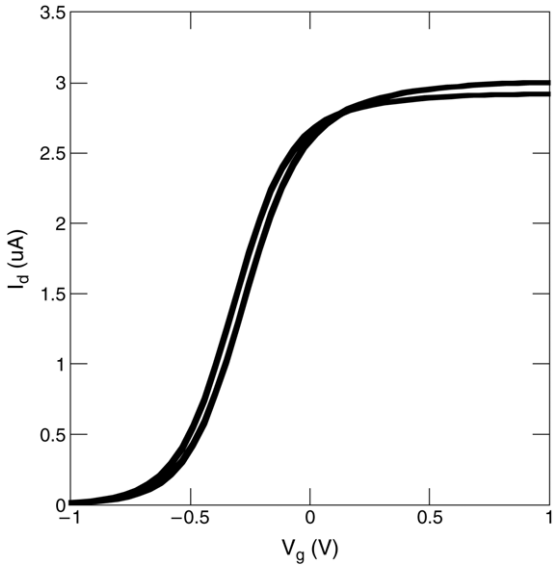

Fig. 1. I_d–V_g characteristics for a doping of 2×10^{18} cm^{-3}. The curves represent two different devices.

utilizing an approach in which the silicon lattice is traversed and dopants are placed in the various regions if a generated random number is less than the ratio between the nominal doping of the region and the volume of silicon atoms in the region [5]. The charge associated with the dopant atoms is then mapped back to the mesh and included in the self-consistent Poisson solution for the potential. This dramatically changes the landscape of the potential as the normally smooth potential variation in the MOSFET is now replaced by a potential profile through which the impinging electron waves must now navigate, through large potential spikes present in the channel, as they traverse from the source to the drain of the device. Moreover, there are large negative spikes in the source and the drain corresponding to the distribution of dopants in those regions. This changes the distribution of the electron density in the source and the drain as there are now energetically preferential sites in the source and the drain for the density. It should be noted that for all devices simulated the drain voltage has been set to $V_d = 10$ meV and the temperature of the system is 300 K.

In the SOI MOSFET under consideration, we have an oversized source and drain region which are doped to 3×10^{19} cm^{-3} n-type. The dimensions of the source and the drain are 18 nm wide, 10 nm long and 6 nm high, corresponding to the thickness of the silicon layer. The source and drain of the device have been given an exaggerated size to exacerbate the interaction of the modes excited in the source with the constriction present at the source–channel interface. The channel of our device is a p-type region. The channel is 10 nm in length, 6 nm in height and 8 nm in width. The I_d–V_g characteristics for a doping of 2×10^{18} cm^{-3} are shown in Fig. 1 for two different devices.

In Fig. 2, we plot the density distribution in the xy-plane for two different gate voltages. In Fig. 2(a), we plot the density in the xy-plane for a gate voltage of -1.0 V which is below threshold. The density is shown at a distance of 3 nm above the bottom of the silicon layer

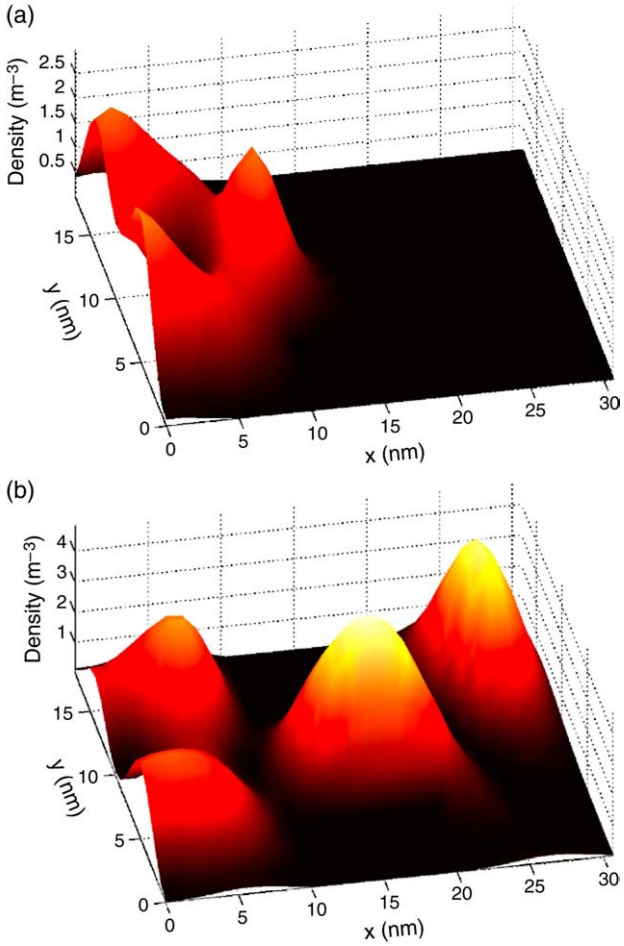

Fig. 2. The density in the xy-plane for a doping of 2×10^{18} cm^{-3} at a distance of 3 nm from the bottom of the silicon layer for a gate voltage of (a) -1.0 V, (b) 1.0 V.

in the device (the center of the channel). As we can see, the vast majority of the excited density is reflected back from both the constriction and the source–channel interface. The reflection is expected as, for this device, the dopants are mainly located at the source side of the channel, thereby providing a better barrier to the density. The nearer the dopants are to the source of the device, the more interaction they have with the source density, without interference from the drain contact. Therefore, the dopants give rise to larger reflections and larger effects on the threshold voltage. Moreover, we find that this reflection forms a standing wave pattern in the x and y directions in the source of the device. We can see that, at this gate voltage, there is virtually no density that is capable of propagating in the channel and, therefore, all of the resulting current is due to the tunneling of the density from the source to the drain.

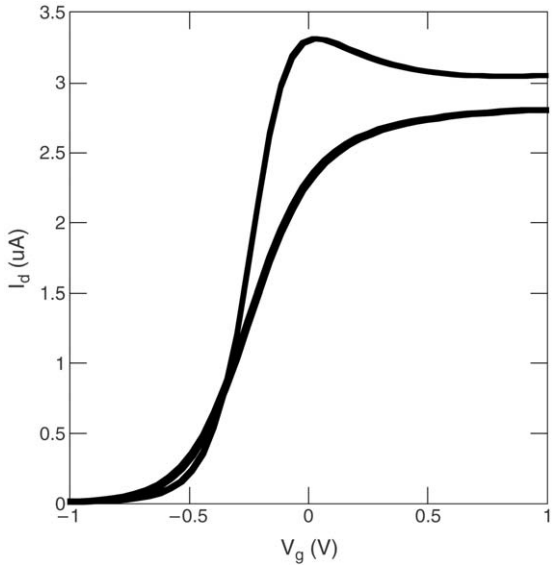

Fig. 3. I_d–V_g characteristics for a doping of 5×10^{18} cm^{-3}. The curves represent two different devices.

In Fig. 2(b), we plot the density in the xy-plane at a distance of 3 nm from the bottom of the silicon layer for a gate voltage corresponding to 1.0 V, which is well above threshold. We now have a fully propagating mode in the channel of the device which has formed a standing wave as the density reflects from the channel–drain opening and interferes with the incident density in the channel. In addition, the density that has exited the channel, which is noticeably less than is present in the source, still forms pools corresponding to the dopant locations in the drain. The resulting current is now saturated at this gate voltage as we have populated the channel with one full mode and the density in the channel is now maximized.

When the doping of the channel is raised from 2×10^{18} to 5×10^{18} cm^{-3}, an additional dopant appears in the channel of the MOSFET. This will add an additional potential spike in the channel potential, which will cause more interference and additional reflections. Therefore, we expect to see more of a discrepancy when we examine the threshold voltages of these devices. In Fig. 3, we plot the I_d–V_g characteristics corresponding to a channel doping of 5×10^{18} cm^{-3} for two devices. There is increased interference due to the inclusion of the additional dopant.

In Fig. 4, we once again plot the resultant densities in the xy-plane for various gate voltages to add additional insight into the resultant curves. In Fig. 4(a), we plot the density in the xy-plane at a distance of 3 nm from the bottom of the silicon layer with a gate voltage of -1.0 V. As in the case of the lighter doping, we find the same type of standing wave pattern in the source. As expected, we see a great deal of reflection from the source–channel barrier and from the constriction. Nevertheless, when we compare this to Fig. 2(a), we find that the density is not quite as peaked at the source–channel barrier as in the previous case. This indicates that, for this sample, the location of the dopants is further in the channel than

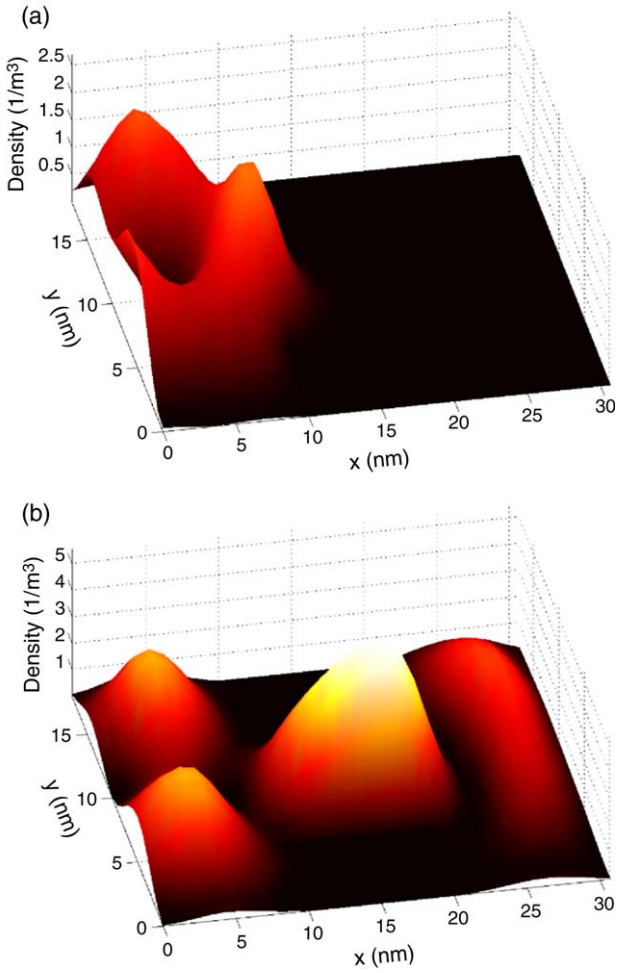

Fig. 4. (a) The density in the xy-plane for a doping of 5×10^{18} cm^{-3} at a distance of 3 nm from the bottom of the silicon layer for a gate voltage of (a) -1.0 V, (b) 1.0 V.

for the previous case. This allows the density to penetrate deeper into the channel before it is reflected. Nevertheless, as in the previous case, all of the current resulting at this gate voltage is due to tunneling from the source to the drain of the device.

In Fig. 4(b) we look at the density in the xy-plane in the device for a gate voltage of 1.0 V. Here we see a great departure from Fig. 2(b) in terms of the form of the channel density and the drain density. In Fig. 4(b), there is much more channel density than in the more lightly doped case and the resultant standing wave pattern is altered from the additional interactions with the channel dopants. The additional interactions then trap more of the density in the channel than is seen in more lightly doped devices. With additional density trapped in the channel of the device, we see that the density that exits the channel is reduced. While it does spread out more smoothly, there is still a variation caused by the

positions of the dopants in the drain. In the case of Fig. 2(b) more of the dopants were concentrated in the corner of the drain causing density to settle there, while in Fig. 4(b) the dopants are more distributed leading to the greater spread of density in the drain.

The position of the dopant atoms has a significant effect on the resultant device characteristics. This is a result of the interference that the potential spikes produce. Dopants that are positioned closer to the source of the device have a greater effect on the threshold voltage than do dopants positioned further down the channel due to increased interaction with the waves incident at the source–channel interface, causing additional reflections. This can produce source–drain resonances as seen in Fig. 3, where two dopants have been positioned at the very boundary between the source and the channel at a depth corresponding to that of maximal density causing a resonant state to form. The fact that the transport properties can be dramatically affected not only by the position in the xy-plane, but also by their position in the z direction, adds additional importance to this work. Further, we see that the positions of the dopants in the source and the drain cause pools of electron density to form. This is again due to the negative potential spikes caused by the donors forming states for the density. This leads to noticeable variation in the density distribution in the source and, particularly, in the drain. All of the preceding features caused by the interaction of the waves with the potential spikes present in the system illustrate the growing importance of the mechanisms of decoherence in ultrashort devices.

Acknowledgement

This work was supported by the Office of Naval Research.

References

[1] R. Chau, 2001 Silicon Nanoelectronics Workshop, Kyoto, Japan, June 10–11, 2001.
[2] B. Yu, H. Wong, A. Joshi, Q. Xiang, E. Ibok, M.-R. Lin, IEDM Tech. Dig. (2001) 937.
[3] B. Doris, M. Ieong, T. Kanarsky, Y. Zhang, R.A. Roy, O. Dokumaci, Z. Ren, F.-F. Jamin, L. Shi, W. Natzle, H.-J. Huang, J. Mezzapelle, A. Mocuta, S. Womack, M. Gribelyuk, E.C. Jones, R.J. Miller, H.-S.P. Wong, W. Hänsch, IEDM Tech. Dig. (2002) 267.
[4] M.J. Gilbert, D.K. Ferry, J. Appl. Phys. (in press).
[5] H.S. Wong, Y. Taur, IEDM Tech. Dig. (1993) 705.